

Research article

DOI: <https://doi.org/10.18721/JCSTCS.18103>

UDC 681.5.08



A TECHNIQUE FOR AUTOMATED ANALYSIS OF THE BLADE SURFACE FOR DEFECTS UNDER UV LIGHT

E.A. Alekseev¹  , A.N. Lomanov²  , D.S. Ivanov¹

¹ PJSC “UEC-Saturn”, Rybinsk, Russian Federation;

² P.A. Solovyov Rybinsk State Aviation Technical University,
Rybinsk, Russian Federation

 evgeny.alekseev@uec-saturn.ru

Abstract. A technique for automated analysis of the blade surface for defects under UV light is presented. The basis of control operations when inspecting blade surfaces is the use of machine vision. The technique solves several key problems: obtaining a package of inspection images of a complex profile object of inspection (an aircraft blade), determining the actual parameters (sizes) of glows for single and group defects, generating expert recommendations (digital trace) for determining the presence of defects on the inspected surfaces for the operator or automated systems. An algorithm for processing images obtained from a video camera is presented, and approaches to compensating for the shift of blades in a frame during inspection rotation are described. The technique describes the following sequentially performed stages: shooting of the blade surface; searching for glows in a two-dimensional image; converting two-dimensional coordinates of the glows into three-dimensional ones; determining the actual parameters of the glows; determining the position of the glows relative to each other; determining the degree of suitability of the blade based on the obtained information about the glows.

Keywords: non-destructive testing, machine vision, technological process automation, measurement systems, recommendation system

Citation: Alekseev E.A., Lomanov A.N., Ivanov D.S. A technique for automated analysis of the blade surface for defects under UV light. *Computing, Telecommunications and Control*, 2025, Vol. 18, No. 1, Pp. 36–47. DOI: 10.18721/JCSTCS.18103

Научная статья

DOI: <https://doi.org/10.18721/JCSTCS.18103>

УДК 681.5.08



МЕТОДИКА АВТОМАТИЗИРОВАННОГО АНАЛИЗА ПОВЕРХНОСТИ ЛОПАТКИ НА НАЛИЧИЕ ДЕФЕКТОВ ПОД УФ-СВЕТОМ

Е.А. Алексеев¹ ✉, А.Н. Ломанов² , Д.С. Иванов¹

¹ ПАО «ОДК-Сатурн», Рыбинск, Российская Федерация;

² Рыбинский государственный авиационный технический университет
имени П.А. Соловьева, Рыбинск, Российская Федерация

✉ evgeny.alekseev@uec-saturn.ru

Аннотация. Представлена методика автоматизированного анализа поверхности лопатки на наличие дефектов под УФ-светом. В основе контрольных операций при осмотре поверхностей лопатки лежит использование машинного зрения. Методика решает несколько ключевых задач: получение пакета инспекционных изображений сложного профильного объекта контроля (авиационной лопатки), определение реальных параметров (размеров) свечений для единичных и групповых дефектов, формирование экспертных рекомендаций (цифрового следа) по определению наличия дефектов на инспектируемых поверхностях для оператора или автоматизированных систем. Приведен алгоритм обработки изображения, получаемого с видеокамеры, описаны подходы по компенсации сдвига лопаток в кадре при инспекционном вращении. Методика описывает следующие последовательно выполняемые этапы: съемка поверхности лопатки, поиск свечений на двумерном изображении, преобразование двумерных координат свечений в трехмерные, определение реальных параметров свечений, определение положения свечений друг относительно друга, определение степени годности лопатки по полученной информации о свечениях.

Ключевые слова: неразрушающий контроль, машинное зрение, автоматизация технологических процессов, системы измерения, рекомендательная система

Для цитирования: Alekseev E.A., Lomanov A.N., Ivanov D.S. A technique for automated analysis of the blade surface for defects under UV light // Computing, Telecommunications and Control. 2025. T. 18, № 1. С. 36–47. DOI: 10.18721/JCSTCS.18103

Introduction

In the aviation industry, methods that help detect surface material discontinuities are widely used during inspection [1, 2–6]. One of them is the capillary method, a non-destructive testing technique [7]. The fluorescent penetrant inspection, being a subtype of this method, exhibits a high sensitivity to the size of defects [8]. The main feature of this type of inspection is filling the surface discontinuities in the material of objects under inspection with fluorescent liquid that has high penetration capability, followed by recording the obtained readings under UV light at the place of the defect visually or using optical devices¹ [9, 10].

The manual implementation of this method, i.e. without the use of automated systems, has a number of disadvantages. The main ones are the following:

- low operating speed (approximately 1 blade per 3 minutes);
- impossibility of performing inspections in the evening and at night due to the reduced attention of flaw detector operators, which significantly reduces the amount of manufactured products.

In order to address the problem of blade surface analysis in this article, a multi-step approach is proposed, which includes the following:

- shooting of the blade surface;

¹ Literature and journals on capillary testing, Available: <https://ndt-testing.ru/literature.html> (Accessed: 18.12.2024)

- searching for indications in a two-dimensional (2D) image;
- converting 2D coordinates of indications into three-dimensional (3D) ones;
- determining the actual parameters of indications;
- determining the position of indications relative to each other;
- determining the degree of suitability of the blade based on the obtained information about the indications.

The defects detected by fluorescent penetrant inspection are very small (from 300 μm) and barely visible, but under UV light they become clearly visible and contrast strongly with the blade surface². Since the defects produce fluorescence in the visible range, for the needs of this article a camera with a CMOS matrix for high-resolution color images was used to detect the defects. The blade should be photographed from different angles to cover its entire surface, for this reason, a device for rotating the blade was used.

Problem formulation and method of solution

When determining the actual shape of indications on the blade surface, the method of converting 2D coordinates of indications into 3D ones, is used. In order to implement this method, the obtained image was compared with the reference image, where each pixel is characterized by its own 3D coordinates on the blade surface [11, 12, 13]. Once all the characteristics of indications were identified, they were classified and the degree of suitability of the blade was determined according to the developed algorithms.

There are many methods for determining the size of objects in an image [14–20]. The main task of all these methods is to identify coordinates of the points of measured objects in 3D space.

The most common methods are based on stereoscopic vision [21–25]. It works like the human eye. The control point, the coordinates of which must be determined, will be in different positions in each camera thereby enabling the system to calculate the position of that point in space. The main advantage of this method are its relative cheapness, a large number of implementations, and the fact that systems using this method can immediately capture high-resolution images (e.g., for data storage). The main disadvantage of this method is that it is necessary to search for pixels representing the same point in two images in order to determine the coordinates of the desired point. If the object being photographed has a monotonous surface, then this search is performed inaccurately, resulting in frequent errors. In this case, an analysis of the blade surface, which is monotonous – gray, would be required. Therefore, this method should not be used in this situation.

In addition to stereoscopic vision, time-of-flight (TOF) cameras can be used [26–29]. The camera illuminates the scene with a modulated light source and observes the reflected light. The phase shift between emission and reflection is then measured and converted into distance. As a result of shooting, the camera provides a distance image for each object. The distances between the desired points can be calculated from the image data. The disadvantage of such cameras is that they do not provide a color image where the defects themselves need to be identified. Therefore, this method requires an additional camera that can capture a colored image of the blade, which is necessary for comparison with the distance image. Furthermore, this method has a relatively low accuracy. The most expensive camera options allow achieving an accuracy of up to 5 mm.

In order to solve the problem, a method is used that, using one camera and a 3D model of an object, will allow determining the size of defects located on its surface [25]. As part of this research of the method for searching the blade surface indications, several problems were solved.

The first problem that needs to be solved to determine the size and position of the indications is finding them in the image. For this purpose, the next obtained image of the blade undergoes multistage processing, namely:

- compensation for the blade shift in the frame;

² Literature and journals on capillary testing, Available: <https://ndt-testing.ru/literature.html> (Accessed: 18.12.2024)

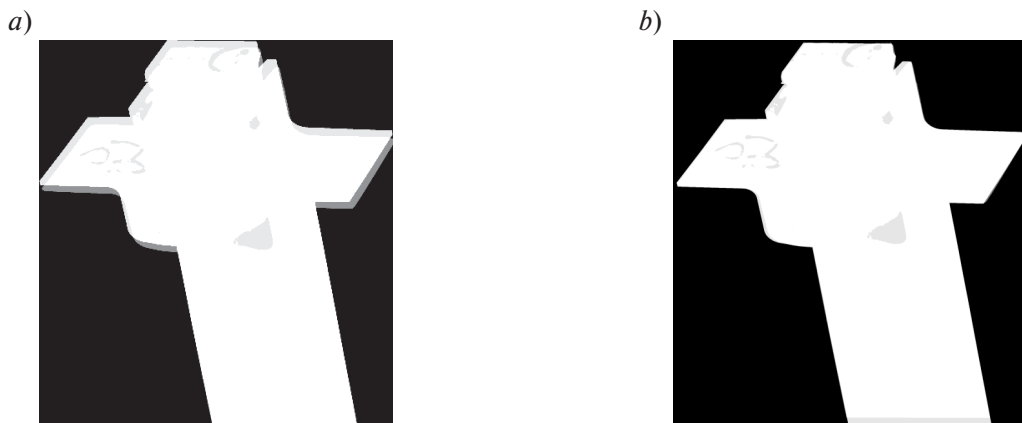


Fig. 1. Result of the blade shift algorithm in the frame:
a) silhouette of the blade before shift relative to the standard;
b) silhouette of the blade after shift relative to the standard

- application of filters that highlight the indication.

First, we determine whether the blade in the frame is shifted relative to the specified position. To do this, its boundaries are calculated using the Canny operator, and then their shift relative to the reference position obtained during the preparation stage is calculated. If the blade in the image is shifted, then it is aligned using affine transformations. If a very large shift is required (more than 2 mm in any direction), then the transformation is not performed, because it may reduce the image detail. The result of the blade shift algorithm in the frame is shown in Fig. 1.

Once the required position has been determined, filters are sequentially applied to the image to highlight the indications, as follows:

- Gaussian blur is applied to suppress noise that may occur due to the use of a color image;
- HSV transformation plus filtering is applied to transform the color palette of a BGR image into HSV; a color threshold filter leaves only those areas that are green;
- threshold filter that enables only bright indications, cutting off the dim ones according to the threshold value;
- morphological transformations (erode and dilate) are used to suppress very small indications (noise), that do not require consideration during analysis;
- clustering plus filtering for clustering of indications using DBSCAN algorithm, determination of median brightness of clusters, filtering by threshold value of median brightness.

After applying the described filters to the image, only the areas with indications remain on it. The indication areas themselves represent an array of pixel coordinates painted white. These areas should be saved and then processed using an algorithm for determining the indication size and position. The result of indication filtering on the image is shown in Fig. 2.

The main problem in determining the size of the indications is that they are located on the surfaces with intricate shape. Each indication in the image is represented by an array of pixels. The size of each array can be calculated, but the values will be obtained in pixels, which do not directly correlate with actual values, for example, millimeters. In addition, all indications are on a curved surface, and the resulting image is 2D, which means that the indications are flat, which does not allow to capture their actual shape. This means that it is practically impossible to calculate the real size and shape of each indication with high accuracy.

In order to solve the problem, image correlation maps are used in the process. For each obtained image, a prepared data set is generated in advance, enabling to correlate each pixel of the image to a point on the blade in 3D space.

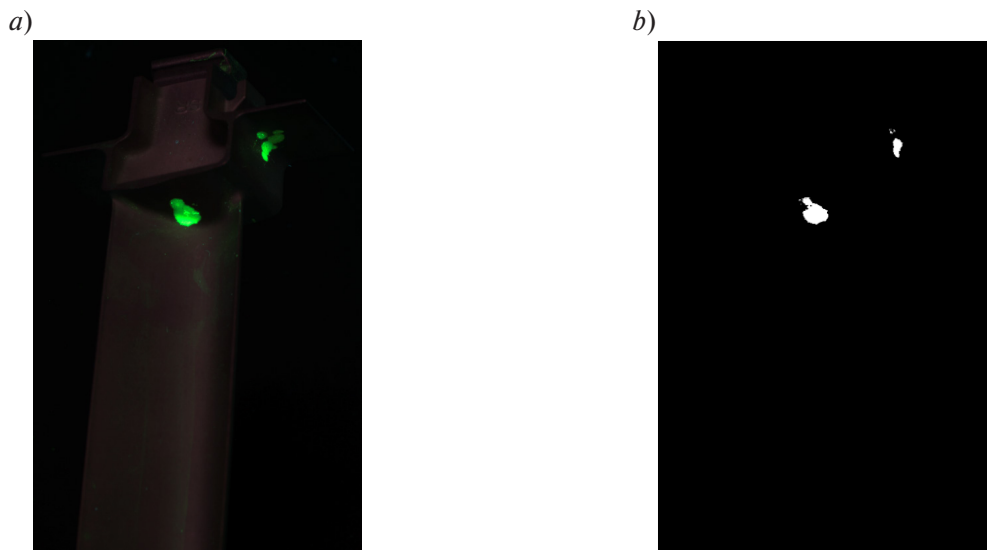


Fig. 2. Result of indication filtering in the image:
 a) image before filtering; b) image after filtering

For the process of generating correlation maps, the developed program was used, which is based on the *OpenGL* specification for simplifying the execution of operations in 3D space. The *PyOpenGL* library is used to implement this specification.

In order to generate an image correlation map for an image, the following steps must be performed:

- 3D pre-zoned model of the blade is loaded into the developed program (the zones are necessary for further analysis);
- 3D scene with the loaded blade model is displayed;
- the camera is positioned in such a manner that the view from the actual image matches that in the scene;
- compilation of a map is launched, which relates the coordinates of each pixel and their coordinates in 3D space.

Thus, image correlation maps are prepared for each position of the blade shooting. This completes the preparatory stage of the work, after which it is possible to launch the algorithm for determining the size of the indications.

The result of this algorithm is an array of indication parameters, namely:

- indication length, mm;
- indication width, mm;
- mean normal vector of indications;
- center of mass of indications;
- blade's number of the zone (or zones) containing an indication;
- distance from the center of mass to its farthest point (radius of the inscribed circle);
- angle between the camera normal and the surface normal (for further calculation of the distance between the indications and duplicates removal);
- coordinates of the square inscribed in the indication in the original image (for further displaying of data to NDT operator).

Specially prepared image correlation maps are used to transform 2D coordinates of indications into 3D ones.

The block diagram of the algorithm of indication parameters identification method is presented in Fig. 3.

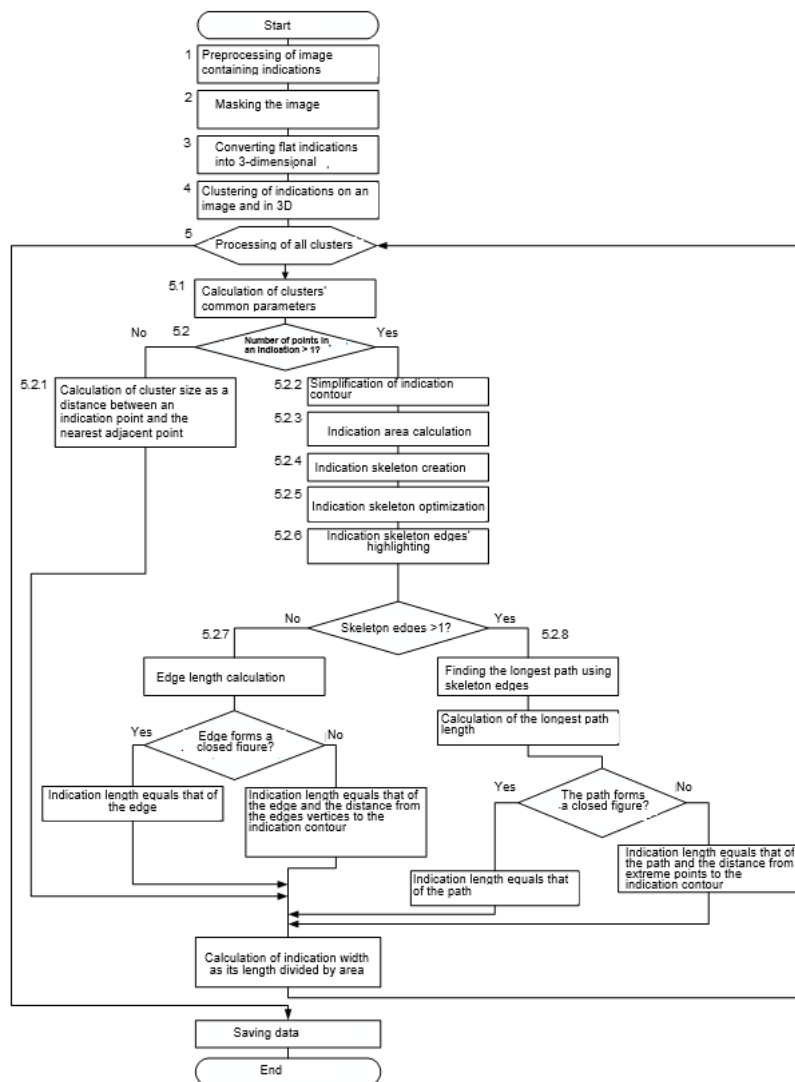


Fig. 3. Algorithm of indication parameters identification method

During digital processing of indication parameters, five main points of the algorithm are consistently implemented:

- 1) image preprocessing;
- 2) masking the image;
- 3) transformation of 2D indications into 3D ones;
- 4) clustering of indications;
- 5) processing of all clusters.

Explanation of each point is given below.

1. The input to the algorithm is a monochromatic image comprising of white areas that serve as indications. In the image, the blade does not take up the entire area, so the area with the blade is cut out. The square area with the blade is cut out to optimize speed and memory space.

2. If indications on the background of the blade were detected (a penetrant drop on the background), they will be ignored. For this purpose, the area obtained in the first step is multiplied by the mask, which is the silhouette of the blade. Thus, only those indications remain that are located on the blade.

3. 2D coordinates of indications are converted into 3D ones according to the prepared image correlation maps.

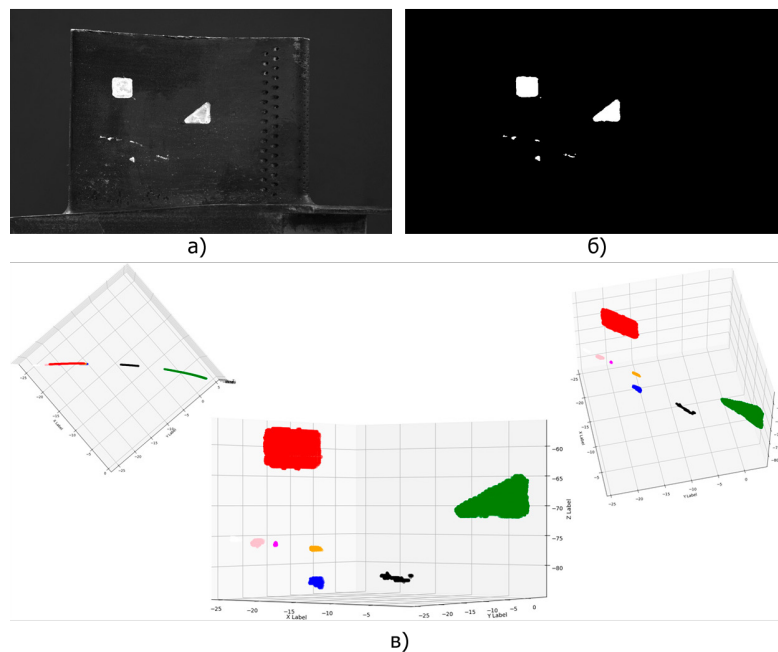


Fig. 4. Algorithm for determining the size and position of indications in graphical form:
 a) original image; b) result of the algorithm for searching for image indications;
 c) result of clustering of defects in 3D space

4. Clustering of indications is performed using DBSCAN algorithm in 2D and 3D space. In 2D space, it is performed in order to merge nearby pixels into one cluster (assumed indication), and then in 3D space – to determine the actual indications and to isolate them.

For 2D clustering, the following parameters are used:

- *eps* (maximum distance between points to form a cluster). The used distance value $\sqrt{2} * 1,05$ is chosen empirically (with the minimum distance between pixels and a slightly greater distance to accommodate diagonal ones, but not to include pixels through which the diagonal passes).
- *min_sample* (minimum number of points to form a cluster). The smallest cluster can consist of 1 point. This number was chosen empirically, based on the fact that very small defects need to be detected.

For 3D clustering, the following parameters are used:

- *eps* – value 1 is used as a distance, which corresponds to 1 mm;
- *min_sample* – the smallest cluster can consist of 1 point.

The result of the first four points of the algorithm is shown in Fig. 4.

Next, the largest section of a 3D cluster (if any) is selected from each 2D cluster. That is, if several indications have merged into one, they will be divided into several clusters in 3D representation, from which the one with the largest number of points will be selected.

5. For all clusters that are periodically processed in the analysis phase, a series of computational procedures is performed.

5.1. Computation of cluster parameters:

- calculation of actual 3D coordinates (clustering taken into account);
- calculation of the center of indications in 3D space (center of mass);
- calculation of coordinates of the extreme point of indications from its center of mass;
- identification of the zone (or zones) on the blade where the indication is found;
- calculation of the normal vector of each point of indications, and calculation of the mean normal vector of indications;

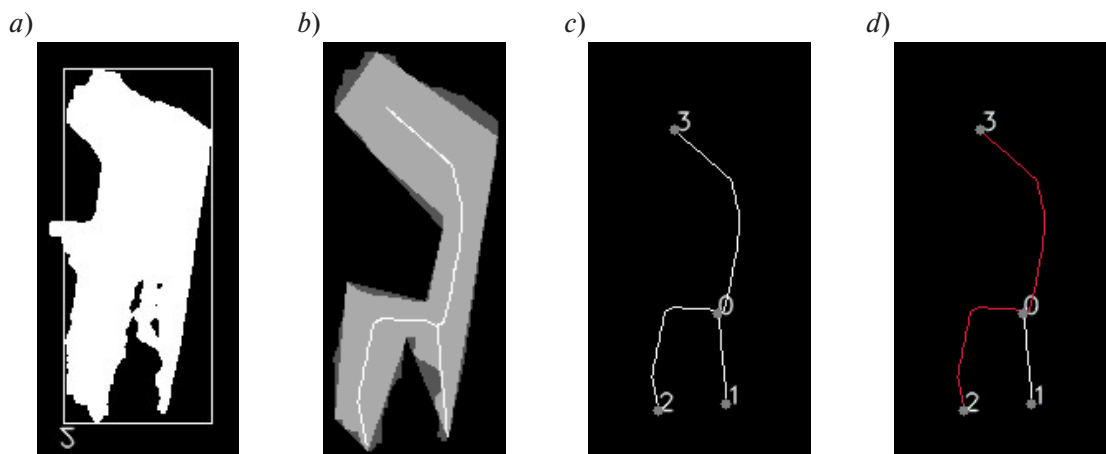


Fig. 5. Visualization of the algorithm for determining the indication length:
a) points forming one cluster (indication); *b)* result of simplification of the indication contour;
c) result of skeletonization of indications; *d)* maximum path that forms the length of indications

- calculation of the angle between the mean normal vector of indications and the normal vector of the camera.

5.2. Next, the geometric dimensions of the indications are calculated:

- indication is represented by a single pixel, its size is considered as the minimum distance to the adjacent pixel. For this purpose, the closest pixel in 3D space is selected from four adjacent pixels;
- if an indication is represented by more than one pixel, its set of points (a list of pixel coordinates) is converted into a binary matrix (image), “cleaned” from various image defects (noise, etc.) using morphological operations. After “cleaning”, the indications contour is determined and simplified by using an approximating function that reduces the number of isolated indication contours (segments) by 25 times.

The coefficient is calculated empirically;

- area and perimeter of the contour (original, not simplified) are calculated;
- simplified contour is re-filled, and then skeletonized, which causes the edges of the binary matrix to erode until only the center lines remain. In some figures, such as a circle, the skeletonizing may leave no points, in which case the point is set at the center;
- the skeleton is processed – the indication skeleton is optimized by excluding all unnecessary points from it;
- skeleton is broken into segments (edges) at the junctions of several branches. The obtained edges are processed, their endpoints and lengths are calculated, deleted points are restored in case of indications skeleton ruptures;
- if, as a result, there is one segment left, that segment is checked to see if it is a closed one. If so, the segment length is used as the length. If the segment is not a closed one, then the distance to the contour is added to its length. In both cases, the width is calculated as the area divided by the resulting length;
- if segments are more than one, the matrix of distances between the vertices of segments is calculated, the longest path from which the length of indications is calculated as the sum of lengths of all segments of the path. Then proceed similarly to previous action.

Fig. 5 provides a visualization of the algorithm for determining the indication length.

All the calculated parameters for each of the indications are stored in one array.

Analysis of the results

When testing the algorithm for determining the size of the defects, it was found that it works best when the surface is inspected perpendicular to the surface. The closer the inspection angle (the smallest angle

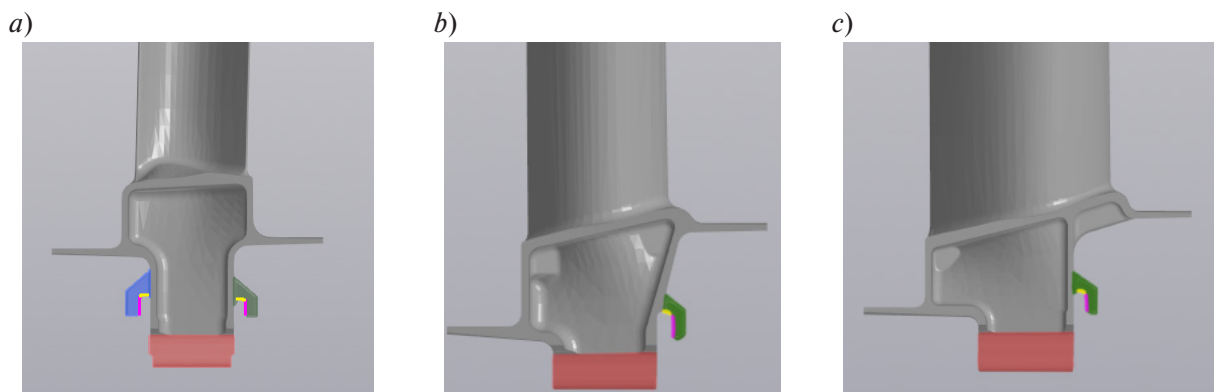


Fig. 6. Blind spots on the blade: a) 2nd stage; b) 3rd stage; c) 4th stage

between the surface plane and the beam from the camera to a point on the surface under inspection) is to 90° , the more accurate are the results. Accordingly, the farther away you go, the less accurate it becomes. This is because the shape of the indications and the surface to be captured are severely deformed when captured at an acute angle. This causes the area of both the surface and the indications in the image to change. This means that the indication starts to occupy a larger area, and therefore its size is calculated incorrectly. In terms of the algorithm, the problem is that when a surface is taken at a right angle, one pixel in the image falls into only one or two polygons on the 3D model, which is used to calculate the size. The smaller the angle of the inspection, the more polygons one pixel starts to occupy, so its size also increases. In this article, areas that cannot be captured at an angle or close to 90° , are called “blind”.

In order to avoid blind spots on the surface of the item under inspection, the following solutions are possible:

- adjust the capture positions so that all surfaces of interest are captured at right angles;
- increase the camera resolution and the number of polygons of the model;
- if possible, inspect hard-to-reach areas of the part separately from the part (e.g. before they are welded together).

An example of difficult to capture zones, as well as “blind” zones, should be given with reference to the blades analyzed in this article. Fig. 6 shows the most difficult areas to inspect, with 2.4.5a showing the 2nd stage, 2.4.5b showing the 3rd stage, and 2.4.5c showing the 4th stage.

The lowest part of the lock (highlighted in red) has a rounded shape and, therefore, its base cannot be captured at a right angle with a single shot. Based on visual analysis of the images, it was concluded that if the number of capture positions is increased, the entire area with the correct viewing angle will be captured.

The hooks on both sides of the lock are the most difficult to capture. The entire outer part of the hooks is captured by the system without any problems (green and dark-blue areas). Inspection of the inner surface of the hooks is particularly difficult.

The lower part (yellow area) is examined in the photo in its entirety, but its viewing angle goes further than 90° , so its measurements are less accurate.

At the inner wall (pink area), the entire area cannot be inspected at right angle, since the lock parts obstruct the view. This surface can only be viewed at an angle of approximately 28° (calculated from 3D model of the blade). This angle is very small to ensure accurate measurements.

Conclusion

When analyzing the blade surface it was found that defects can be detected, classified and sized on 98% of the surface area using machine vision. In the yellow and pink areas, defects are visible, but it is difficult to classify and size defects using automated methods, because the 90° viewing angle cannot be

maintained according to the procedure. The probability of defects in these zones has not been assessed, however, according to the consultation with the NDT operators, defects in the yellow and pink zones are detected not more than once per 100–200 defective blades. The size of defects is determined visually by the NDT operator, referring to the standard.

Based on the analysis we can conclude that it is possible to use machine vision based automated control means to identify defects under UV light. Sizing of defects from 100 microns is possible. The problem of impossibility of sizing the defects in “blind” spots can be solved by rejection of parts containing any detected indications.

REFERENCES

1. Byrkov I.A., Vyzhletsov V.V., Kozhanov N.Yu., Mishin S.A., Okov I.N. *Method for processing images by convolutional neural networks*. Patent Russia No. RU 2771442 C1, 2020.
2. Nesterov A.V. *Programmno-apparatnyj kompleks mashinnogo zreniya dlya opredeleniya i kontrolya shiriny mezhvitkovogo zazora [Machine vision hardware and software system for determining and controlling the width of the interturn gap]*. Patent Russia No. RU 126490 U1, 2013.
3. Kilian K., Mazur V., Fan K. *System for machine vision, which enables to determine depth non-uniformity of image objects*. Patent Russia No. RU 2604168 C2, 2016.
4. Ono K., Tate M. *Method for detecting surface defects, device for detecting surface defects, method for producing steel materials, method for steel material quality control, steel materials production plant, method for generating models for determining surface defects and a model for determining surface defects*. Patent Russia No. RU 2764644 C1, 2022.
5. Nigmatullin F.T., Sorvin I.I. *Method of non-destructive optical and visual testing of items by means of computer vision*. Patent Russia No. RU 2777718 C1, 2022.
6. Li C., Li L., Jiang H., Weng K., Geng Y., Li L., Ke Z., Li Q., Cheng M., Nie W., Li Y., Zhang B., Liang Y., Zhou L., Xu X., Chu X., Wei X., Wei X. YOLOv6: A single-stage object detection framework for industrial applications, 2022. DOI: 10.48550/arXiv.2209.02976
7. Poletaev V.A. *Tekhnologiya avtomatizirovannogo proizvodstva lopatok gazoturbinnih dvigatelej [Technology of automated production of gas turbine engine blades]*. Moscow: Mashinostroenie, 2006. 256 p.
8. Glazkov Yu.A. *Kapillyarnyj kontrol' [Capillary testing]*. Moscow: ID Spektr, 2011. 144 p.
9. Kalinichenko N.P., Kuleshov V.K., Kalinichenko A.N. *Kontrol' kachestva pronikayushchimi veshchestvami. Kapillyarnyj kontrol' [Quality control by penetrants. Capillary testing]*, 2nd ed. Tomsk: Izd-vo Tomskogo politekhnicheskogo universiteta, 2007. 203 p.
10. Popko E.A., Vorob'ev A.P., Vainshtein I.A. Experience of machine vision application in optical NDT systems. *Svarka i diagnostika: sbornik dokladov mezhdunarodnogo foruma [Welding and diagnostics: collection of reports of the international forum]*, 2015, Pp. 401–406.
11. Egunov O.V., Hartasenko A.V., Chepchurov M.S. *Ustrojstvo beskontaktnogo izmereniya sherohovatosti poverhnoy detalej slozhnoj formy [Device for non-contact measurement of surface roughness of complex-shaped parts]*. Patent Russia No. RU 104697 U1, 2011.
12. GitHub – ultralytics/ultralytics: Ultralytics YOLO11, Available: <https://github.com/ultralytics/ultralytics> (Accessed: 19.12.2024)
13. Sychev I.E. Avtomaticheskaya sistema raspoznavaniya defektov na baze tekhnicheskogo zreniya [Automatic defect recognition system based on machine vision]. *Al'ternativnaya i intellektual'naya energetika: Materialy II Mezhdunarodnoj nauchno-prakticheskoy konferencii [Alternative and Intelligent Energy: Proceedings of the II International Scientific and Practical Conference]*, 2020, Pp. 18–19.
14. Ermakov A.A. *Metody i algoritmy obrabotki i analiza snimkov v kapillyarnoj defektoskopii. Avtoref. kand. tekhn. nauk. [Methods and algorithms for processing and analyzing images in capillary flaw detection. Cand. tech. sci. diss.]*. Vladimir, 2009. 19 p.

15. Shipway N.J., Barden T.J., Huthwaite P., Lowe M.J.S. Automated defect detection for Fluorescent Penetrant Inspection using Random Forest. *NDT & E International*, 2019, Vol. 101, Pp. 113–123. DOI: 10.1016/j.ndteint.2018.10.008
16. Shipway N.J., Huthwaite P., Lowe M.J.S., Barden T.J. Using ResNets to perform automated defect detection for Fluorescent Penetrant Inspection. *NDT & E International*, 2021, Vol. 119, Article no. 102400. DOI: 10.1016/j.ndteint.2020.102400
17. Tout K. *Automatic Vision System for Surface Inspection and Monitoring: Application to Wheel Inspection. PhD thesis*. Troyes, 2018. 188 p.
18. Bobkov A.V. Intercepting Image in Problem of Orientation by Visual Information. *Herald of the Bauman Moscow State Technical University. Series Instrument Engineering*, 2002, Vol. 48, No. 3. Pp. 45–54.
19. Aust J., Shankland S., Pons D., Mukundan R., Mitrovic A. Automated defect detection and decision-support in gas turbine blade inspection. *Aerospace*, 2021, Vol. 8, Article no. 30. DOI: 10.3390/aerospace8020030
20. Wang C.-Y., Bochkovskiy A., Liao H.-Y. M. YOLOv7: Trainable bag-of-freebies sets new state-of-the-art for real-time object detectors, 2022. DOI: 10.48550/arXiv.2207.02696
21. Gonzalez R.C., Woods R.E. *Digital image processing*, 3rd ed. London: Pearson, 2007. 976 p.
22. Soifer V.A. *Computer Image Processing, Part II: Methods and algorithms*. Riga: VDM Verlag Dr. Müller, 2010. 584 p.
23. Priorov A.L., Khriashchev V.V., Topnikov A.I. *Obrabotka i peredacha mul'timedijnoj informacii [Processing and transmission of multimedia information]*. Yaroslavl: Yaroslavskij gosudarstvennyj universitet im. P.G. Demidova, 2022. 248 p.
24. Korotaev V.V., Krasnyashchih A.V. *Televizionnye izmeritel'nye sistemy [Television measuring systems]*. St. Petersburg: SPbGU ITMO, 2008. 108 p.
25. Korneichuk V.S., Kotlyar D.I., Lomanov A.N., Medvedev E.Yu. *Application of machine vision for calculating defect sizes during fluorescent penetrating testing of gas turbine engine blades*. Bulletin of the Cherepovets State University. Cherepovets: Cherepovets State University, 2022, No. 1 (106), Pp. 31–41. DOI: 10.23859/1994-0637-2022-1-106-3
26. Kazakov O.D., Romashov N.E. Real-time object detection and recognition using a machine learning model. *Vyzovy cifrovoj ekonomiki: razvitie komfortnoj gorodskoj sredy [Challenges of the digital economy: development of a comfortable urban environment]*, 2020, Pp. 353–356.
27. Yamshchikov S.A. Komp'yuternoe zrenie v nerazrushayushchem kontrole [Computer vision in non-destructive testing]. *Novye materialy, oborudovanie i tekhnologii v promyshlennosti: Materialy Mezhdunarodnoj nauchno-tekhnicheskoy konferencii molodyh uchenyh [New Materials, Equipment and Technologies in Industry: Proceedings of the International Scientific and Technical Conference of Young Scientists]*, 2021, P. 163.
28. Chikmarev D.D., Habarov A.R., Karelskaya K.A. Computer vision system for objects defectoscopy. *Informacionnye resursy i sistemy v ekonomike, nauke i obrazovanii: sbornik statej XI Mezhdunarodnoj nauchno-prakticheskoy konferencii [Information Resources and Systems in Economics, Science and Education: proceedings of the XI International Scientific and Practical Conference]*, 2021, Pp. 171–174.
29. Forsyth D., Pons J. *Computer vision: A modern approach*, 2nd ed. London: Pearson, 2011. 800 p.

INFORMATION ABOUT AUTHORS / СВЕДЕНИЯ ОБ АВТОРАХ

Alekseev Evgeny A.
Алексеев Евгений Александрович
 E-mail: evgeny.alekseev@uec-saturn.ru

Lomanov Alexey N.
Ломанов Алексей Николаевич
 E-mail: frei@rsatu.ru
 ORCID: <https://orcid.org/0000-0001-9271-1552>

Ivanov Dmitry S.
Иванов Дмитрий Станиславович
E-mail: dmitry.ivanov@uesc-saturn.ru

Submitted: 12.06.2024; Approved: 02.09.2024; Accepted: 20.12.2024.

Поступила: 12.06.2024; Одобрена: 02.09.2024; Принята: 20.12.2024.